

Supporting Information for

Singlet and Triplet Excitation Management in a Bichromophoric Near-Infrared-Phosphorescent BODIPY–Benzoporphyrin Platinum Complex

Matthew T. Whited, Peter I. Djurovich, Sean T. Roberts, Alec C. Durrell,[†] Cody W. Schlenker, Stephen E. Bradforth, and Mark E. Thompson*

Department of Chemistry, University of Southern California, Los Angeles, California 90089

Derivation of Equation 1	S2
Figure S1. ¹ H NMR spectrum of Pt(^{BDP} TPBP) (4) in CDCl ₃	S3
Figure S2. UV/Vis of H ₄ (^{BDP} TPCHP) (2).....	S4
Figure S3. UV/Vis of Pt(^{BDP} TPCHP) (3).....	S5
Figure S4. Excitation ($\lambda_{em} = 760$ nm) and emission ($\lambda_{ex} = 410$ nm) spectra of 3 at 77 K in 2-MeTHF	S6
Figure S5. Excitation ($\lambda_{em} = 765$ nm) and emission ($\lambda_{ex} = 438$ nm) spectra of 4 at 77 K in 2-MeTHF	S7
Figure S6. Excitation ($\lambda_{em} = 768$ nm) and emission ($\lambda_{ex} = 435$ nm) spectra of 4 doped (0.5%) into a PMMA film	S8
Figure S7. UV/Vis of Pt(^{BDP} TPBP) (4) as a neat film	S9
Figure S8. Excitation ($\lambda_{em} = 935$ nm) and emission ($\lambda_{ex} = 450$ nm) spectra of 4 as a neat film at 77 K..	S10
Figure S9. UV/Vis of Me ₂ BODIPY model complex in CH ₂ Cl ₂	S11
Figure S10. Excitation ($\lambda_{em} = 575$ nm) and emission ($\lambda_{ex} = 350$ nm) spectra of Me ₂ BODIPY model complex in CH ₂ Cl ₂	S12
Figure S11. UV/Vis of Pt(TPBP) model complex in CH ₂ Cl ₂	S13
Transient Absorption of Pt(^{BDP}TPCHP) (3)	S14
Figure S12. Ultrafast transient absorption spectra of 3 after excitation at 515 nm (0.2–5 ps).....	S14
Figure S13. Ultrafast transient absorption spectra of 3 after excitation at 515 nm (5–300 ps).	S15

Derivation of Equation 1.

The Boltzmann distribution describes the non-normalized probability that a state of a given energy will be occupied at a given temperature.

For a two-state system, where P_n denotes the fractional population of state n and d_n denotes the degeneracy of state n , the following ratio will hold true:

$$\frac{d_1 \cdot e^{-E_1/kT}}{d_1 \cdot e^{-E_1/kT} + d_2 \cdot e^{-E_2/kT}} = \frac{P_1}{P_1 + P_2} = P_1$$

Take the inverse of both sides:

$$\frac{1}{P_1} = \frac{d_1 \cdot e^{-E_1/kT} + d_2 \cdot e^{-E_2/kT}}{d_1 \cdot e^{-E_1/kT}} = \frac{d_1 \cdot e^{-E_1/kT}}{d_1 \cdot e^{-E_1/kT}} + \frac{d_2 \cdot e^{-E_2/kT}}{d_1 \cdot e^{-E_1/kT}} = 1 + \frac{d_2}{d_1} \cdot e^{(E_2 - E_1)/kT}$$

Replacing $E_2 - E_1$ with ΔE and rearranging affords:

$$\frac{1}{P_1} - 1 = \frac{1 - P_1}{P_1} = \frac{P_2}{P_1} = \frac{d_2}{d_1} \cdot e^{\Delta E/kT}$$

Multiplying through by (d_1/d_2) , taking the natural log of both sides, and further rearranging gives:

$$\Delta E = E_2 - E_1 = kT \cdot \ln\left(\frac{d_1 P_2}{d_2 P_1}\right)$$

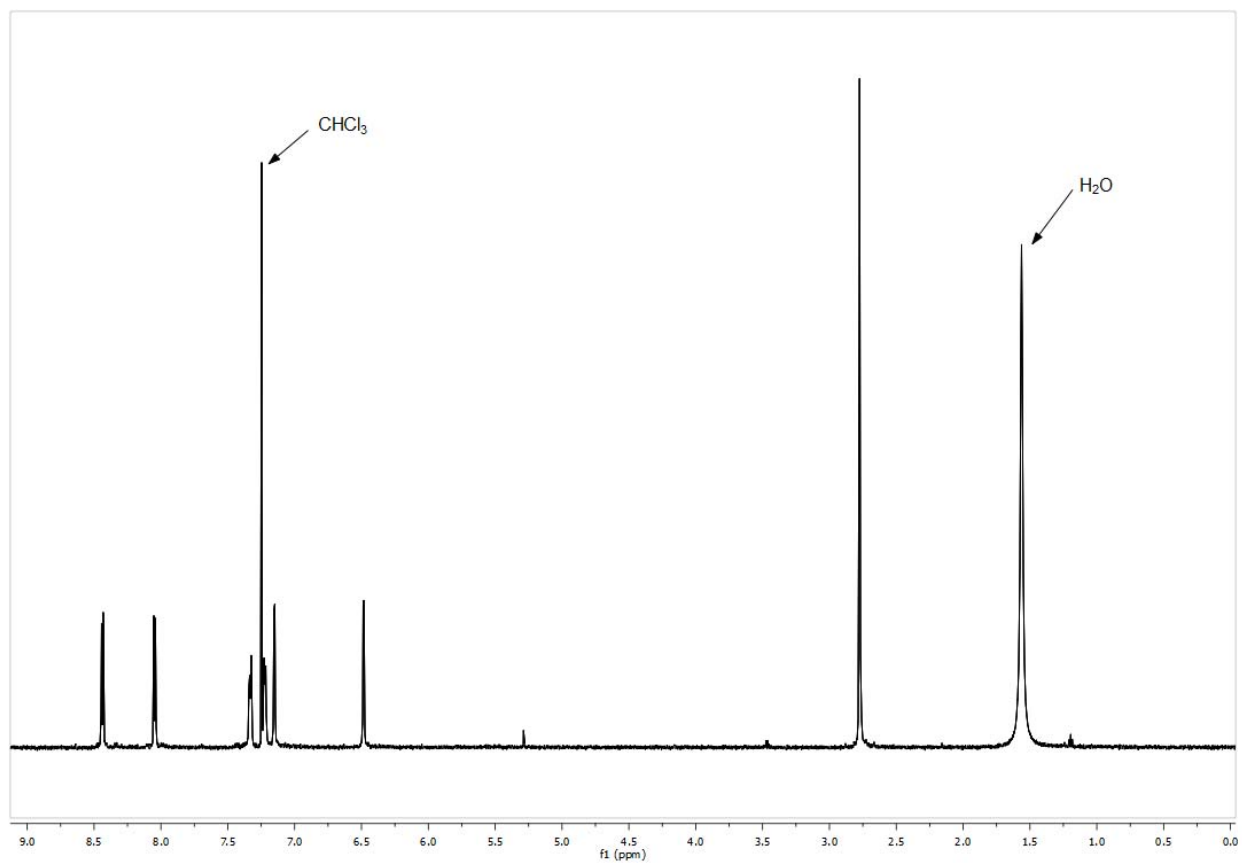


Figure S1. ^1H NMR spectrum of $\text{Pt}(\text{BDP})\text{TPBP}$ (**4**) in CDCl_3 .

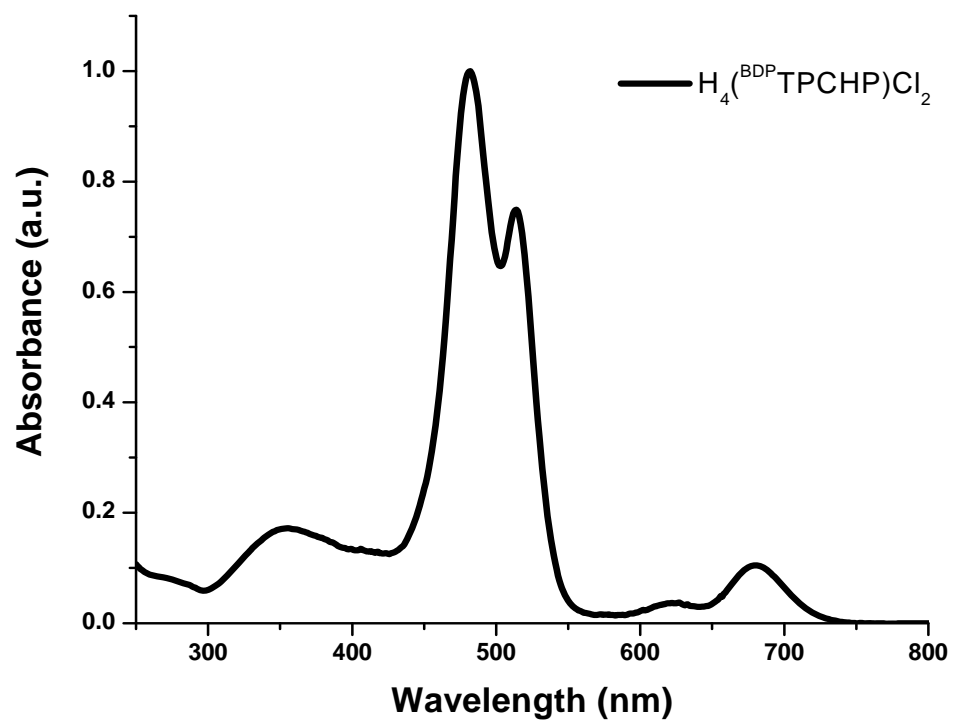


Figure S2. UV/Vis of $H_4(BDP-TPCHP)$ (**2**).

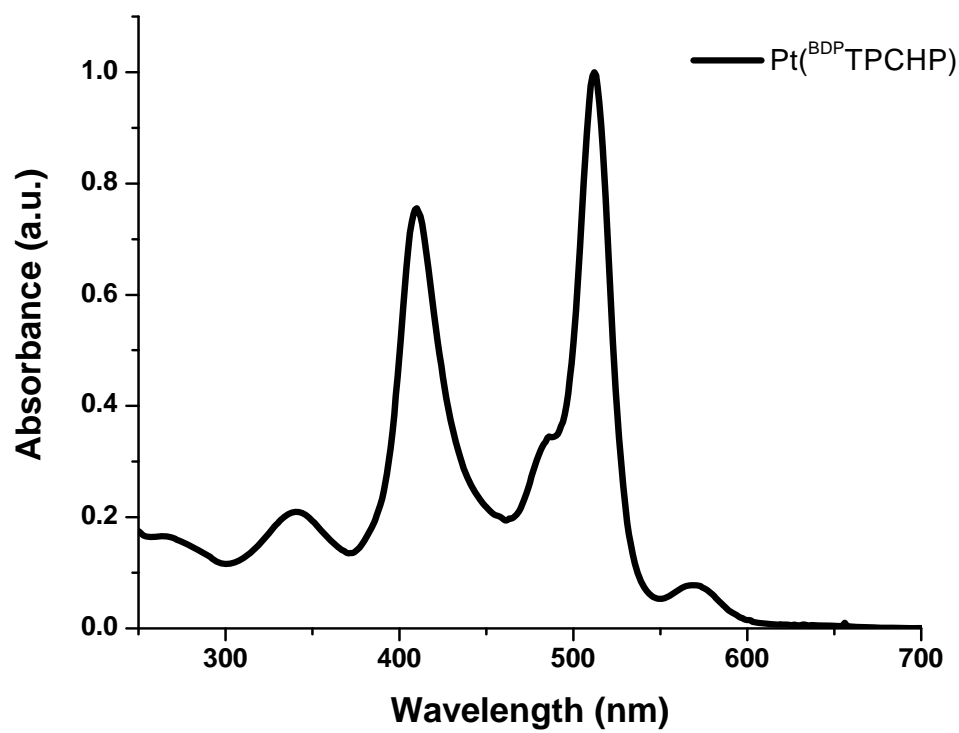


Figure S3. UV/Vis of Pt(BDP)TPCHP (3).

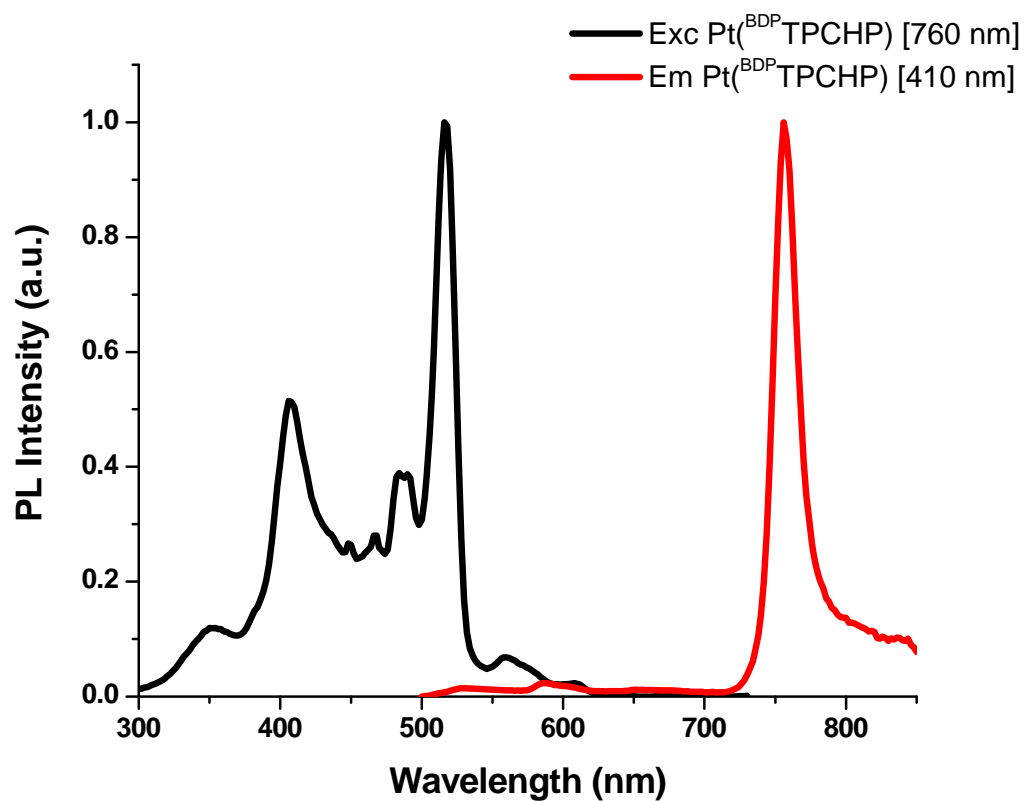


Figure S4. Excitation ($\lambda_{em} = 760$ nm) and emission ($\lambda_{ex} = 410$ nm) spectra of **3** at 77 K in 2-MeTHF.

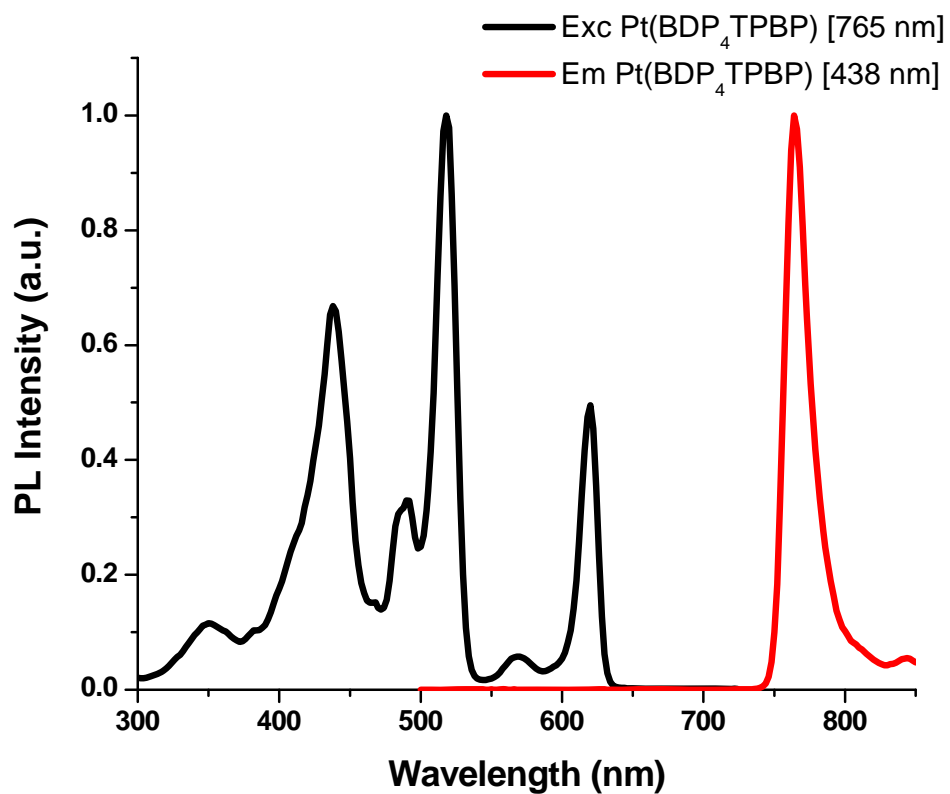


Figure S5. Excitation ($\lambda_{em} = 765$ nm) and emission ($\lambda_{ex} = 438$ nm) spectra of **4** at 77 K in 2-MeTHF.

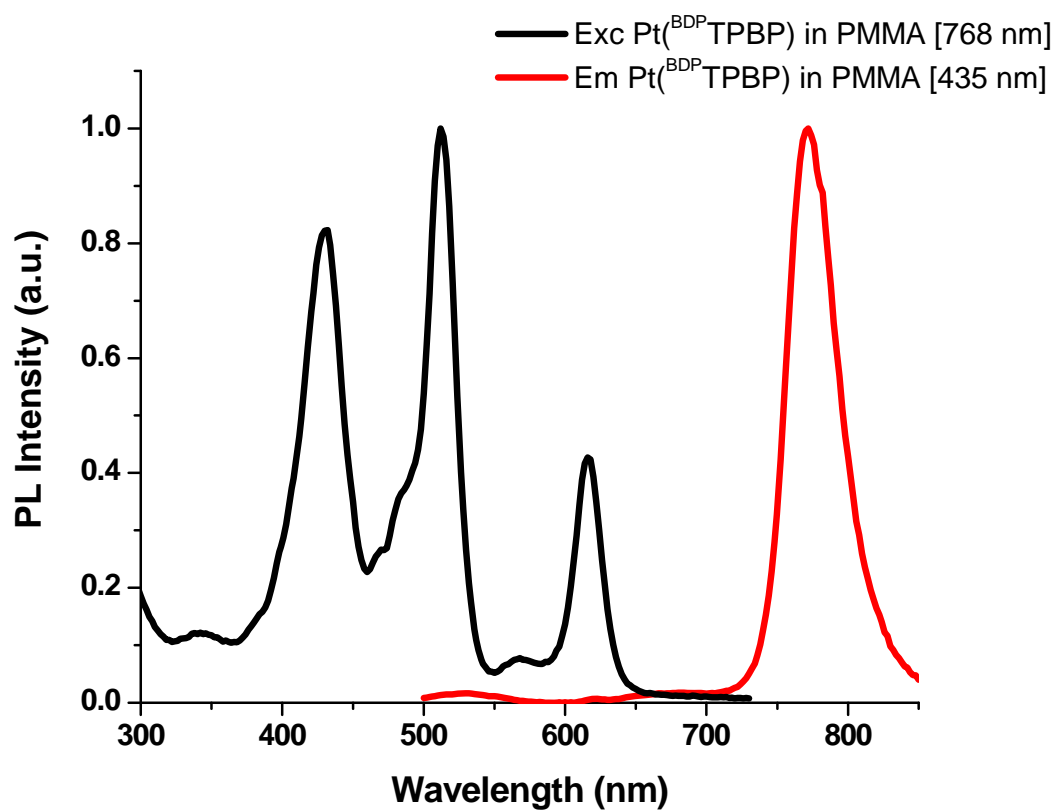


Figure S6. Excitation ($\lambda_{em} = 768$ nm) and emission ($\lambda_{ex} = 435$ nm) spectra of **4** doped (0.5%) into a PMMA film.

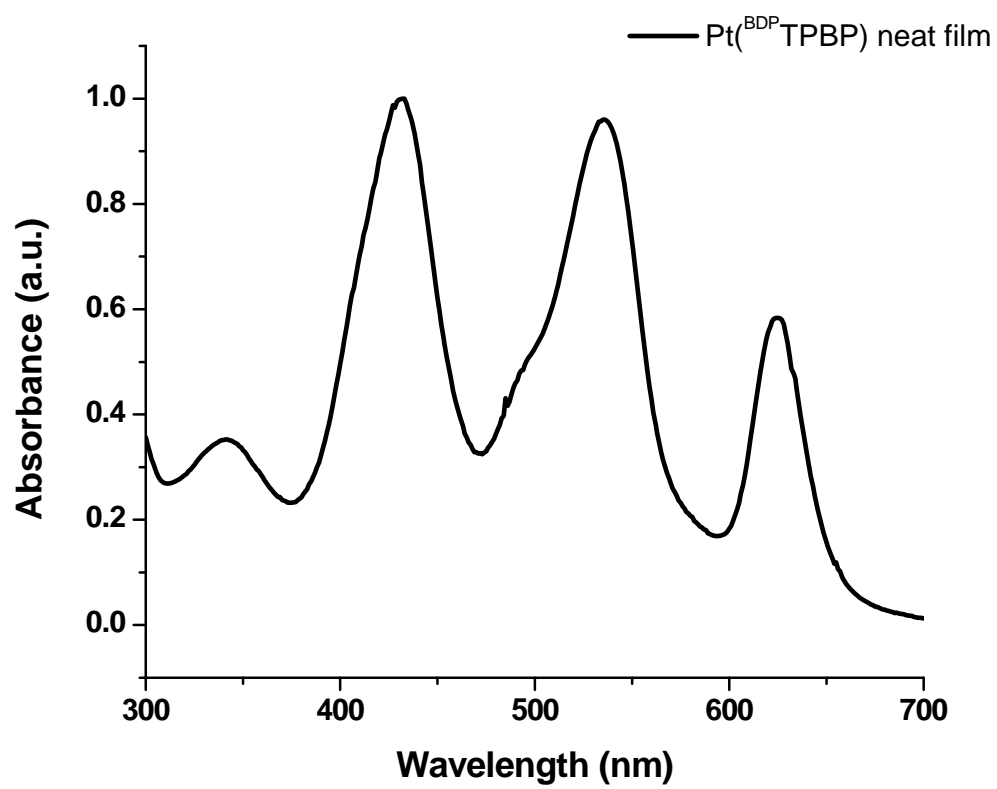


Figure S7. UV/Vis of Pt(^{BDP}TPBP) (**4**) as a neat film.

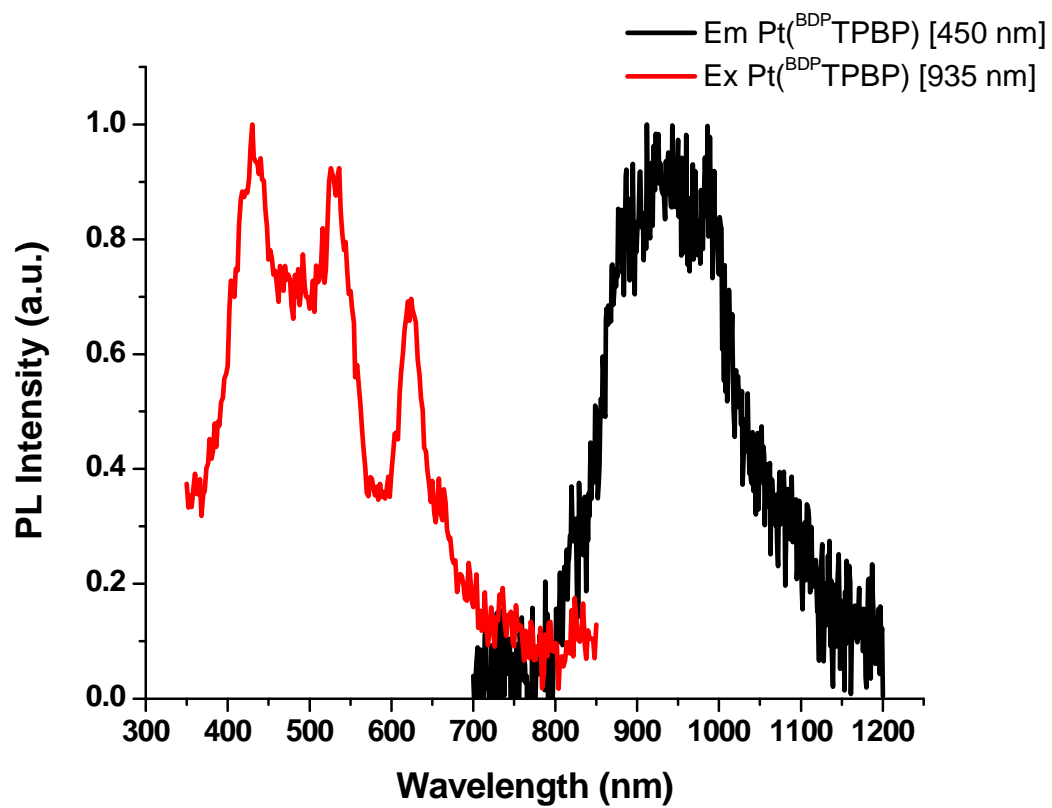


Figure S8. Excitation ($\lambda_{em} = 935$ nm) and emission ($\lambda_{ex} = 450$ nm) spectra of **4** as a neat film at

77 K.

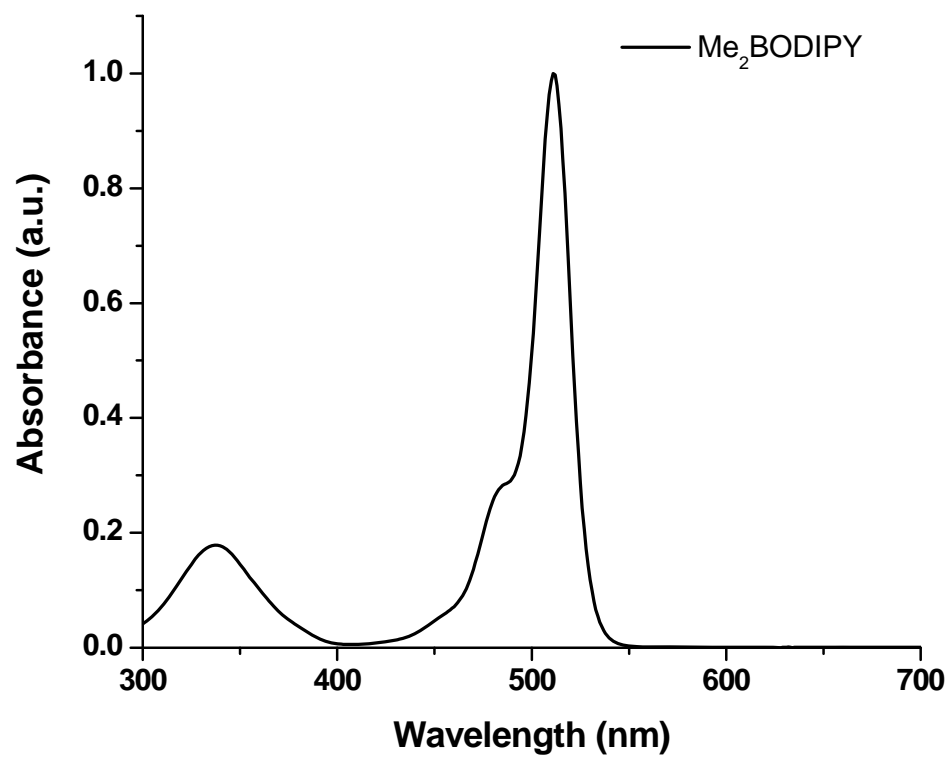


Figure S9. UV/Vis of Me₂BODIPY model complex in CH₂Cl₂.

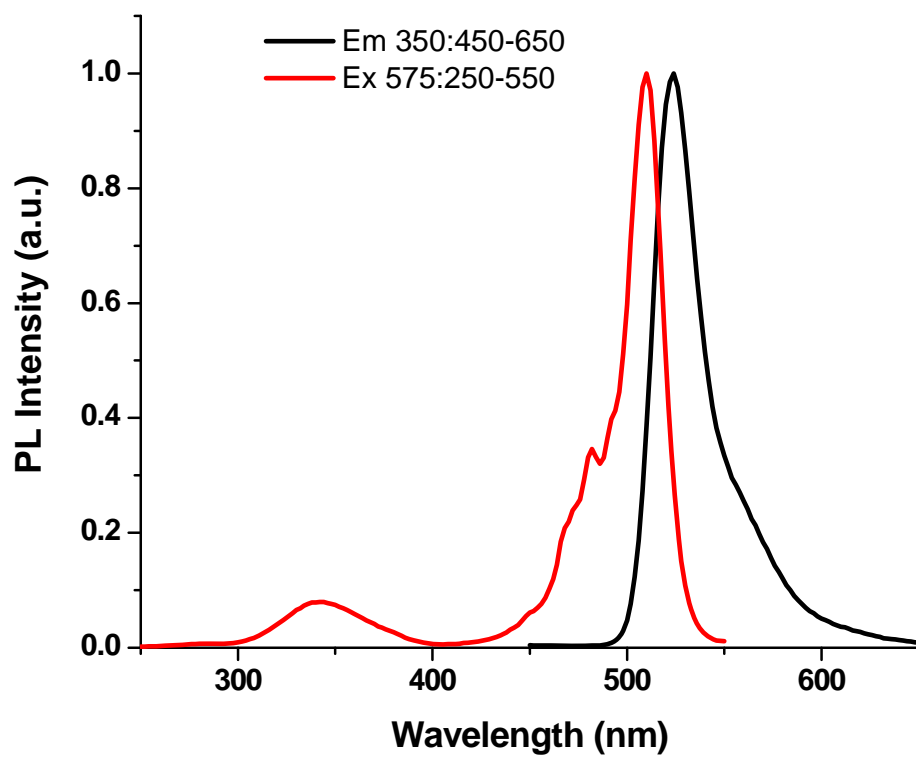


Figure S10. Excitation ($\lambda_{em} = 575$ nm) and emission ($\lambda_{ex} = 350$ nm) spectra of Me₂BODIPY model complex in CH₂Cl₂.

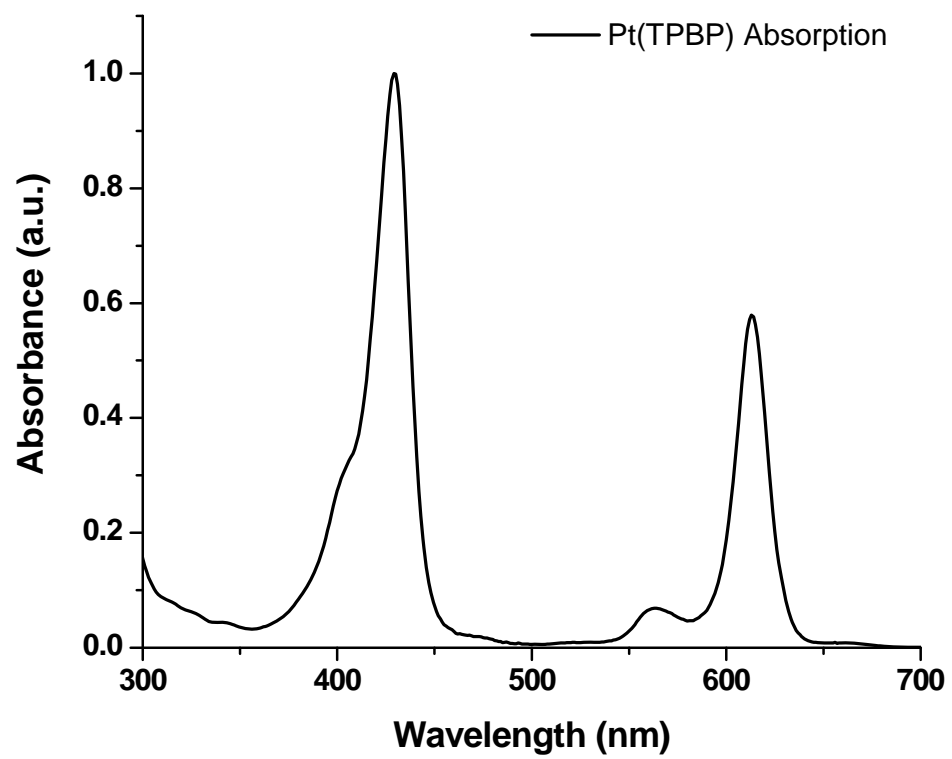


Figure S11. UV/Vis of Pt(TPBP) model complex in CH₂Cl₂.

Transient Absorption of Pt(^{BDP}TPCHP) (**3**).

The transient absorption spectrum of ³BDP could be estimated from the transient absorption of Pt(^{BDP}TPCHP) (**3**), for which the BODIPY triplet is significantly lower in energy than the porphyrin triplet. Upon irradiation of the BODIPY unit ($\lambda = 515$ nm), ¹BDP is immediately generated. As with benzoporphyrin **4** (reported in manuscript), Förster resonant energy transfer (FRET) occurs in picoseconds to generate ¹Por ($k_{ST}^{-1} = 1.20 \pm 0.19$ ps), as shown in Figure S12. Fast intersystem crossing ($k_{ISC}^{-1} < 1$ ps) converts ¹Por to ³Por, causing the cyclohexenoporphyrin triplet to be almost exclusively observed after 5 ps.

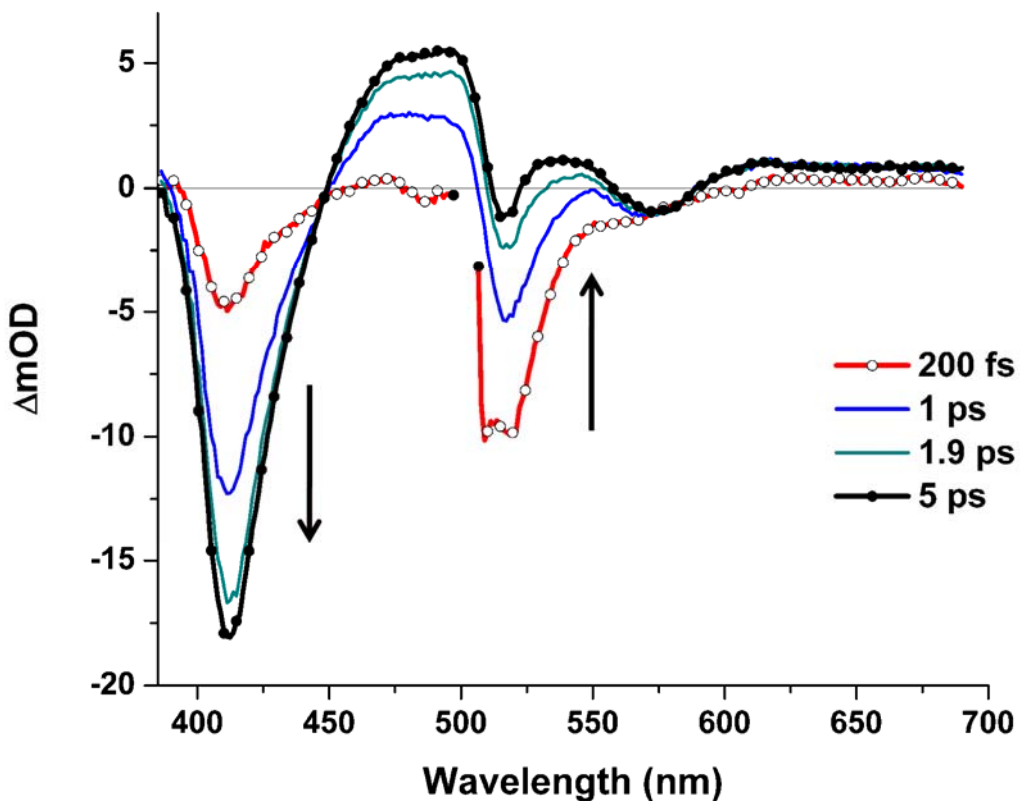


Figure S12. Ultrafast transient absorption spectra of **3** in toluene after excitation at 515 nm (0.2–5 ps) (n.b., solvent response at short time delays prevents the accurate collection of data from 480–500 nm, so these data points have been omitted from the 200 fs trace above).

On slightly longer time scales, triplet energy transfer occurs from ^3Por to ^3BDP ($k_{\text{TT}}^{-1} = 37.0 \pm 4.7$ ps, a rate that is comparable to that for **4**) (Figure S13). Since the BODIPY triplet is significantly lower in energy than the cyclohexenoporphyrin triplet of **3**, the *transient absorption spectrum obtained after 300 ps is derived almost exclusively from generation of ^3BDP* (Figure S13, black trace).

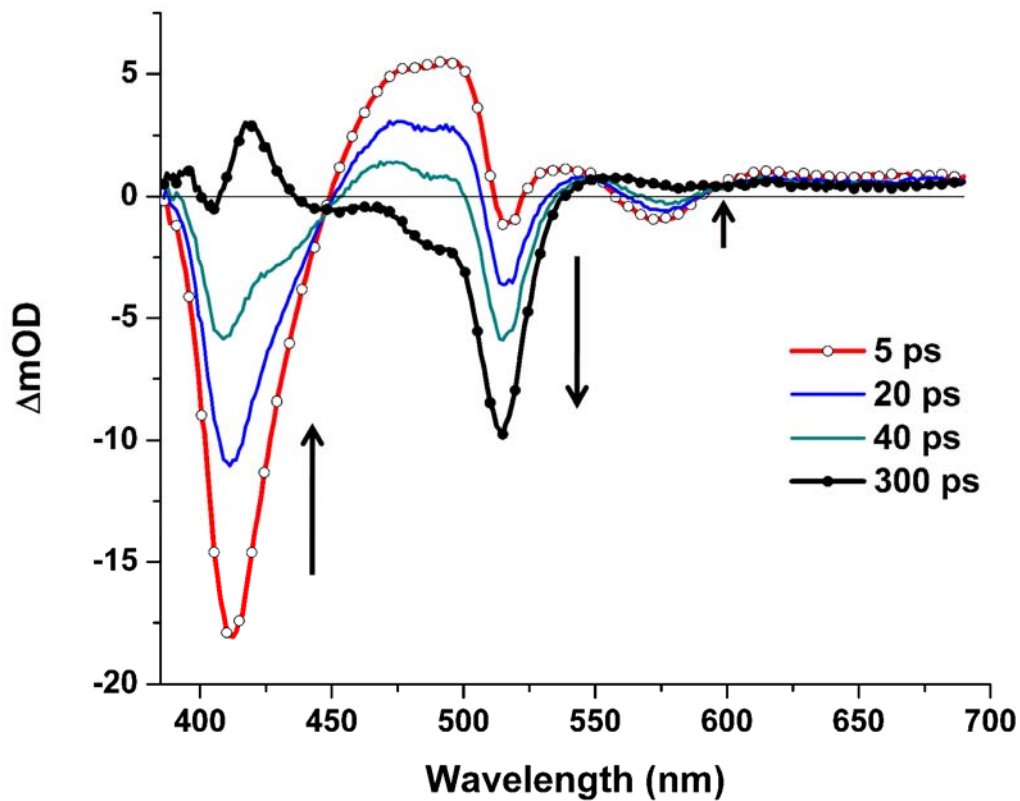


Figure S13. Ultrafast transient absorption spectra of **3** in toluene after excitation at 515 nm (5–300 ps).